

UDK/UDC: 532: 556.32(282)

Prejeto/Received: 18.12.2023

Izvirni znanstveni članek – *Original scientific paper*

Sprejeto/Accepted: 23.02.2024

DOI: [10.15292/acta.hydro.2023.06](https://doi.org/10.15292/acta.hydro.2023.06)

Objavljeno na spletu/Published online: 18.03.2024

TWO-DIMENSIONAL UNCONFINED SEEPAGE FLOW TOWARD A HIGHWAY CUT SLOPE

DVODIMENZIONALNI TOK PODZEMNE VODE S PROSTO GLADINO PROTI AVTOCESTNEMU VKOPU

Yebegaeshet T. Zerihun¹

¹ David & James – Engineering and Environmental Consultancy, 204 Albion Road, Victoria 3350, Australia

Abstract

The unconfined gravity-flow system near a free-outflow boundary such as a highway cut slope was investigated by using a higher-order numerical model. Unlike the Dupuit–Forchheimer equation, which is applicable mainly to a hydraulic flow problem, the proposed model accounts for the effects of the vertical component of the flow for a full treatment of the problem of plane phreatic flow. The model equations were numerically solved by means of a finite-difference scheme. Their accuracy was then verified using the solutions of the full two-dimensional potential-flow method and rigorous mathematical approaches, revealing that for a face slope flatter than 70° , the differences between the solutions of the model and the earlier approaches for the relative seepage-face height were nearly negligible. The comparison results also demonstrated the substantial effects of the slope of the downstream face on this height and the seepage discharge. Furthermore, the accuracies of the model predictions for the phreatic-surface profile and the distributions of the piezometric head at different vertical sections are much better than the earlier method, which approximates the trapezoidal-shaped aquifer by its equivalent rectangular one. Such a satisfactory performance may be attributed to the model's higher-order correction factor for the effects of the phreatic-surface curvature and steep slope.

Keywords: unconfined seepage flow, phreatic surface, artificial cut, seepage discharge, non-hydrostatic groundwater flow, seepage-face height.

Izveček

Z numeričnim modelom višjega reda je bil raziskan gravitacijski tok pri prosti gladini v bližini meje prostega odtoka, kot je na primer vkop avtoceste. Za razliko od Dupuit–Forchheimerjeve enačbe, ki se uporablja predvsem za hidravlični tok, predlagani model upošteva vplive vertikalne komponente toka za celovito obravnavo problema ravninskega toka vode pri prosti gladini. Enačbe modela toka so bile numerično rešene s pomočjo diferenčne sheme. Natančnost rešitve je bila preverjena ob upoštevanju dvodimenzionalnega toka in s strogimi matematičnimi pristopi. Za naklone vkopa, ki je položnejši od 70° , so razlike v višini vode na precejnem robu med rešitvami tega modela in prejšnjimi pristopi skoraj zanemarljive. Primerjava rezultatov

¹ Stik / Correspondence: zyebegaeshet@gmail.com

© Zerihun Y.; This is an open-access article distributed under the terms of the [Creative Commons Attribution – NonCommercial – ShareAlike 4.0 Licence](https://creativecommons.org/licenses/by-nc-sa/4.0/).

© Zerihun Y.; Vsebina tega članka se sme uporabljati v skladu s pogoji [licence Creative Commons Priznanje avtorstva – Nekomercialno – Deljenje pod enakimi pogoji 4.0](https://creativecommons.org/licenses/by-nc-sa/4.0/).

je prav tako pokazala na znatne vplive naklona vkopa na višino vode na precejnem robu in odtok. Poleg tega je natančnost modelne napovedi za potek gladine podzemne vode in porazdelitev hidravličnih višin na različnih navpičnih odsekih veliko boljša od prejšnje metode, ki vodonosnik trapezne oblike upošteva kot ekvivalentni pravokotni vodonosnik. Zadovoljivo rešitev je možno pripisati modelnemu korekcijskemu faktorju višjega reda za učinke ukrivljenosti gladine podzemne vode in strmega pobočja.

Ključne besede: precejanje pri prosti gladini, gladina podzemne vode, vkop, odtok, nehidrostatsko precejanje, višina vode na precejnem robu.

1. Introduction

The analysis of unconfined saturated flow began with the work of Dupuit (1863), who developed a simple but useful model of groundwater flow by considering only the horizontal flow conditions and ignoring the processes occurring in the vertical direction. The Dupuit approach assumed that the horizontal length scale of a typical unconfined aquifer is much larger than the vertical length (Bear et al., 1968, p. 191). As a result, the energy losses associated with the horizontal flow process dominate the total losses within the saturated aquifer. The Dupuit approach was later generalized by Forchheimer (1886, 1914). It is obvious that the Dupuit–Forchheimer (DF) approach is applicable mainly to a hydraulic flow problem where the streamlines are nearly horizontal. In the case of an unsaturated-saturated gravity-flow system near the free-outflow boundary such as a stream bank or a highway cut slope, the vertical component of the flow cannot be ignored. For this flow situation, the DF approach does not predict the presence of a seepage-face boundary at the groundwater-surface water interface (see, e.g., Muskat, 1946, p. 362). The existence of a seepage face provides the necessary transition between the internal phreatic surface and the external equipotential boundaries. Several investigators (e.g. Hall, 1955; Vauclin et al., 1979; Billstein, 1998; Chapman and Ong, 2006) utilized the physical model tests to better understand the characteristics of the unconfined flow near a seepage-face boundary. The results of such tests were also used to fine tune the performance of various types of numerical models. The development of a higher-order numerical model capable of simulating a seepage-flow scenario, where vertical flow component and seepage-face formation are significant, is the task of this study.

In the past, many researchers proposed higher-order approaches to analyzing unconfined groundwater-flow problems. Dagan (1967) was probably the first to develop second-order governing equations for unsteady groundwater flow by applying a procedure expanding in powers of a small parameter. His approach accounted for the effects of the vertical component of the flow. Based on the assumption of a quadratic variation of a piezometric (hydro-potential) head across a vertical section, Kashef (1969) proposed simplified equations for a steady unconfined groundwater flow by analyzing the hydrodynamic forces within the flow medium. The results of the equations for discharge and seepage-face height were compared with rigorous mathematical solutions, demonstrating improved accuracy over the DF approach. For a homogeneous and isotropic aquifer with a sloping downstream face, however, his method provides neither analytical nor numerical solutions to the phreatic-surface profile and the hydro-potential distribution. Using a similar assumption for the profile of the piezometric head, Knight (2005) proposed approximate solutions to the unconfined seepage-flow problems. Muleshkov and Banerjee (1987) employed conformal mapping techniques to obtain a solution to the problem of the two-dimensional (2D) steady-state seepage flow. However, the practical application of their analytical solution is restricted by the assumption of infinite flow domains. As an alternative, Chapman and Dressler (1984) proposed governing equations in a bed-fitted curvilinear coordinate system for a transient unconfined groundwater flow over curved impermeable bedrock. Using the assumption of a small bedrock curvature, Chapman and Ong (2006) developed a simplified version of the Chapman and Dressler flow profile equation for a non-hydrostatic shallow groundwater flow. Their equation can be

retrieved from the Hilberts et al. (2004) equation by considering flow in a constant-width aquifer. Since the bedrock curvature is incorporated without resorting to higher-order terms in the shallowness expansion, the resulting governing equations of these studies do not separate the effects of the phreatic-surface curvature from the bedrock curvature and become identical to the DF equation for the case of mild-slope planar bedrock. The Picard iteration method, which was originally proposed by Matthew (1991) for open-channel flow, was employed by Castro-Orgaz and Hager (2014) to extend the DF approach. Using the power series expansion of the harmonic stream function (Boussinesq, 1871; Rayleigh, 1876) and Darcy's law, Di Nucci (2018) developed a higher-order differential equation for a curved unconfined flow over horizontal impermeable bedrock. Additionally, the numerical solutions of this equation for 2D seepage flow through a rectangular-shaped dam were investigated, and the results of the phreatic-surface profile showed satisfactory agreement with the numerical test data. Zerihun (2018) presented a higher-order approach for analyzing curvilinear groundwater flow in a constant-width unconfined aquifer. His method allowed for the effect of non-hydrostatic pressure, thereby overcoming the limitations of the DF approach. More recently, this approach was extended to deal with unconfined flows in convergent- and divergent-type hillslope aquifers with non-uniform bedrock slopes (Zerihun, 2020). Although those equations had relatively long and complicated non-linear coefficients, they yielded reasonably accurate solutions to the problems of groundwater flow with a phreatic surface.

This study was undertaken to address some of the above deficiencies by developing an alternative numerical model for a 2D unconfined groundwater flow. The field of interest is the problem of a steady-state phreatic flow through a homogeneous aquifer with a slanting side cut, which is commonly encountered along highways and railways (see Figure 1). For this type of flow problem, approximate analytical solutions based on a complex potential-flow theory (e.g. Polubarinova-Kochina, 1962, pp. 301-308; Kacimov and

Obnosov, 2012) and the results of the empirical methods (e.g. Kozeny, 1931; Casagrande, 1937; Fukuchi, 2018) are available. From the computational point of view, however, the evaluation of some of the resulting formulas is not straightforward. In comparison, the proposed model is simple to use and has a higher-order correction term for the effects of the phreatic-surface curvature. As a result, it allows the treatment of complex unconfined flow behaviors that may influence the predictions of seepage discharge, phreatic-surface profiles, and seepage-face height, and obviates the deficiencies of some of the existing models. The model's capacity for analyzing the salient features of a non-hydrostatic seepage-flow problem is also investigated by comparing its numerical solutions with the results of the full 2D potential-flow method and rigorous mathematical approaches. The complete solutions of the unconfined flow problem considered here are relevant for assessing the long-term stability of the slope of a highway cut section. In the following sections, the derivation of the governing equations and the development of the numerical solution procedure based on a finite-difference approximation will be presented.



Figure 1: A steeply sloping side cut along the curved section of a highway (Photograph courtesy of ROADEX Network, Finland).

Slika 1: Strm vkop vzdolž zakrivljenega odseka avtoceste (fotografija z dovoljenjem ROADEX Network, Finska).

2. Governing equations

The flow problem under consideration is a groundwater flow in an unconfined aquifer over curved impermeable bedrock with a steep slope. Figure 2 shows a schematic of the groundwater-flow problem in a Cartesian coordinate system, where x is horizontal in the streamwise direction; y is vertically upward; and z is horizontal in the lateral direction. The following assumptions are made to derive the equations using the Matthew (1991) step-wise iterative approach: (1) the variations of flow parameters in the transverse direction are ignored; (2) the aquifer is isotropic and homogeneous; and (3) the capillary fringe effects are ignored.

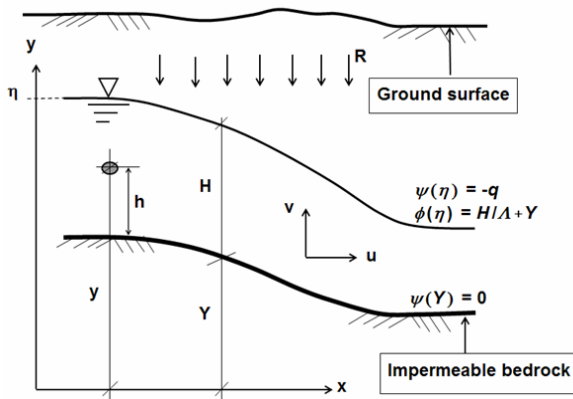


Figure 2: Definition sketch of curvilinear groundwater flow with a phreatic surface.

Slika 2: Definijska skica krivolinijskega toka podzemne vode z gladino podzemne vode.

The first approximation corresponds to the lowest-order equation of an unconfined groundwater flow in a sloping aquifer. For such a gradually-varied flow, the expression for the piezometric or hydraulic head is given by (Zerihun, 2018)

$$\phi(x, \xi, t) = \frac{H(1-\xi)}{\Lambda} + \frac{H\xi}{\Lambda} + Y, \quad (1a)$$

$$\xi = \frac{y-Y}{\eta-Y}, \quad (1b)$$

where η refers to the phreatic-surface elevation; H is the saturated thickness of the aquifer; y is the elevation of a point in the flow field; Y is the bedrock elevation; $\phi(= y + p/\gamma)$ is the piezometric

head or the potential function; p is the pressure; γ is the unit weight of the fluid; ξ is the dimensionless vertical height; t is the time; and $\Lambda = 1 + (Y_x)^2 + H_x Y_x$.

Applying Darcy's law to Equation (1a) results in

$$u = -K \frac{\partial \phi}{\partial x} = -K \left(\frac{H_x}{\Lambda} + Y_x \right), \quad (2)$$

where u is the velocity in the streamwise x -direction, and K is the average hydraulic conductivity of a saturated aquifer. In the above and succeeding equations, the subscript x denotes partial differentiation with respect to the horizontal x -axis. Subsequent corrections can be applied to Equation (2) using the following Cauchy–Riemann conditions (Bear, 1988, p. 234):

$$u = -K \frac{\partial \phi}{\partial x} = -\frac{\partial \psi}{\partial y}, \quad (3)$$

$$v = -K \frac{\partial \phi}{\partial y} = \frac{\partial \psi}{\partial x}, \quad (4)$$

where ψ is the stream function, and v is the vertical velocity. For simplifying the algebraic manipulation, the vertical height above the bedrock $h(= y - Y)$ is used hereafter (see Figure 2). Based on this simple approach, Equation (3) is integrated with the aid of Equation (2) to give the following first-order approximation for the stream function:

$$\psi(x, \xi, t) = -\int u dh = KH \left(\frac{H_x}{\Lambda} + Y_x \right) \xi + \omega_1(x, t), \quad (5)$$

where ω_1 is a function of integration. Imposing the boundary condition at the bedrock ($\psi = 0$) results in $\omega_1 = 0$. Differentiating Equation (5) with respect to x yields an equation for the vertical velocity as follows:

$$v = \frac{\partial \psi}{\partial x} = KH \left(\frac{H_{xx}}{\Lambda} + Y_{xx} \right) \xi - KY_x \left(\frac{H_x}{\Lambda} + Y_x \right). \quad (6)$$

Substituting the above equation into Equation (4) and integrating the resulting expression with respect to h gives the following higher-order approximation for the potential function:

$$\phi(x, \xi, t) = -\frac{1}{K} \int v dh = -\frac{H^2}{2} \left(\frac{H_{xx}}{\Lambda} + Y_{xx} \right) \xi^2 + Y_x H \left(\frac{H_x}{\Lambda} + Y_x \right) \xi - \frac{\omega_2(x, t)}{K}, \quad (7)$$

where ω_2 is a function of integration. According to Matthew (1991), two approaches can be utilized to determine the expressions for this function. The first one is by imposing the dynamic boundary condition at the phreatic surface, $p(\xi=1)=0$, which results in the following equation for ϕ :

$$\phi(x, \xi, t) = H^2 \left(\frac{H_{xx}}{\Lambda} + Y_{xx} \right) \left(\frac{1-\xi^2}{2} \right) - Y_x H \left(\frac{H_x}{\Lambda} + Y_x \right) (1-\xi) + \left(\frac{H}{\Lambda} + Y \right). \quad (8)$$

This higher-order equation accounts for the curvilinear nature of the phreatic flow in the vertical plane, and hence it can accurately describe the distribution of the piezometric head across the saturated depth. The second approach applies the boundary conditions of the stream function at the bedrock and phreatic surface. For this purpose, Equation (7) is first inserted into Equation (3) and then differentiated with respect to x . This results in a higher-order approximation for the horizontal velocity component as follows:

$$u = -K \frac{\partial \phi}{\partial x} = \frac{KH^2}{2} \left(\frac{H_{xxx}}{\Lambda} + Y_{xxx} \right) \xi^2 - 2KHY_x \left(\frac{H_{xx}}{\Lambda} + Y_{xx} \right) \xi - KHY_{xx} \left(\frac{H_x}{\Lambda} + Y_x \right) \xi + KY_x^2 \left(\frac{H_x}{\Lambda} + Y_x \right) + \frac{\partial \omega_2}{\partial x}. \quad (9)$$

Integration of Equation (9) with respect to h leads to the desired higher-order approximation for the stream function, i.e.

$$\psi(x, \xi, t) = -\int u dh = -\frac{KH^3}{6} \left(\frac{H_{xxx}}{\Lambda} + Y_{xxx} \right) \xi^3 + KH^2 \left(Y_x \left(\frac{H_{xx}}{\Lambda} + Y_{xx} \right) + \frac{Y_{xx}}{2} \left(\frac{H_x}{\Lambda} + Y_x \right) \right) \xi^2 - KHY_x^2 \left(\frac{H_x}{\Lambda} + Y_x \right) \xi + \frac{\partial \omega_2}{\partial x} H \xi + \omega_3(x, t), \quad (10)$$

where ω_3 is also a function of integration. The expressions for ω_3 and $\partial \omega_2 / \partial x$ are obtained by applying the boundary conditions $\psi(\xi=0)=0$ and $\psi(\xi=1)=-q$, respectively, and are given by:

$$\omega_3 = 0, \quad (11)$$

$$\frac{\partial \omega_2}{\partial x} = -KH \left(\frac{H}{6} \left(\frac{H_{xxx}}{\Lambda} + Y_{xxx} \right) - Y_x \left(\frac{H_{xx}}{\Lambda} + Y_{xx} \right) \right) + K \left(\frac{HY_{xx}}{2} - Y_x^2 \right) \left(\frac{H_x}{\Lambda} + Y_x \right) + \frac{q}{H} = 0, \quad (12)$$

where q is the discharge per unit width. Substituting the above equations into Equation (10) and simplifying the resulting expression yields the following equation:

$$\psi(x, \xi, t) = \frac{KH^3}{6} \left(\frac{H_{xxx}}{\Lambda} + Y_{xxx} \right) (\xi - \xi^3) + KH^2 Y_x \left(\frac{H_{xx}}{\Lambda} + Y_{xx} \right) (\xi^2 - \xi) + \frac{KH^2 Y_{xx}}{2} \left(\frac{H_x}{\Lambda} + Y_x \right) (\xi^2 - \xi) - q \xi. \quad (13)$$

By making use of Equation (12) in Equation (9), an expression for the distribution of the horizontal velocity is obtained as follows:

$$u = \frac{KH^2}{6} \left(\frac{H_{xxx}}{\Lambda} + Y_{xxx} \right) (3\xi^2 - 1) + KHY_x \left(\frac{H_{xx}}{\Lambda} + Y_{xx} \right) (1 - 2\xi) + \frac{KHY_{xx}}{2} \left(\frac{H_x}{\Lambda} + Y_x \right) (1 - 2\xi) + \frac{q}{H}. \quad (14)$$

Similar to the results of previous studies (e.g. Chapman and Dressler, 1984; Di Nucci, 2018; Zerihun, 2018, 2020), this equation includes terms that account for the effects of the vertical curvature

of the streamline. Substituting Equation (8) in Equation (3) and equating the resulting expression to Equation (14) yields the following flow profile equation for an unconfined groundwater flow:

$$\begin{aligned} & \frac{H^2}{3} \left(\frac{H_{xxx}}{\Lambda} + Y_{xxx} \right) + HH_x \left(\frac{H_{xx}}{\Lambda} + Y_{xx} \right) \\ & - \frac{HY_{xx}}{2} \left(\frac{H_x}{\Lambda} + Y_x \right) - \left(H_x Y_x + Y_x^2 \right) \left(\frac{H_x}{\Lambda} + Y_x \right) \\ & + \left(\frac{H_x}{\Lambda} + Y_x \right) + \frac{q}{KH} = 0. \end{aligned} \quad (15)$$

The above equation implicitly incorporates not only the effects of non-uniform horizontal velocity and non-hydrostatic pressure distributions but also the effect of a steep bedrock slope for accurately modeling the problems of a groundwater flow with a phreatic surface. Thus, it differs from previous equations (e.g. Castro-Orgaz and Hager, 2014; Di Nucci, 2018) developed by the Boussinesq (1871) or Matthew (1991) approach. For a 2D unconfined saturated flow on a vertical plane, the depth-averaged mass-conservation equation reads as (Bear, 1988, p. 376):

$$\lambda \frac{\partial H}{\partial t} + \frac{\partial}{\partial x} \left(\int_0^H u dh \right) = \lambda \frac{\partial H}{\partial t} + \frac{\partial q}{\partial x} = R, \quad (16)$$

where λ is the effective porosity of the aquifer, and R is the rate of vertical recharge. For a curvilinear groundwater-flow problem, the variation of the phreatic-surface profile can be predicted by combining the above depth-averaged continuity equation with Equation (15). Additionally, the present approach gives complete solutions for the rate of seepage flow, height of the seepage surface, and hydro-potential distribution within the saturated region. In the case of phreatic flows with streamlines nearly parallel to the sloping planar bedrock, Equation (15) reduces to:

$$H \left(\frac{H_x}{\Lambda} + Y_x \right) + \frac{q}{K} = 0, \quad (17)$$

which is a Boussinesq-type equation developed by Childs (1971) and was adapted by Chapman (1980) for analyzing the phreatic-surface profiles. For horizontal bedrock, this equation degenerates to the DF equation for steady groundwater flow with no

recharge. Because of the non-linear characteristics of Equations (15) and (16), closed-form solutions are not possible except in highly simplified cases. In this study, a numerical approach based on the finite-difference approximations was employed to solve the equations. Using such a relatively simple numerical technique, the applicability of the proposed equations is systematically investigated for the test cases of non-hydrostatic seepage flows towards artificial cuts ($\Lambda = 1$). Such transient types of flow problems may be approximately analyzed by a quasi-steady flow approach, ignoring the aquifer's storage capacity and the time lag between the inflow and outflow peak discharges.

3. Seepage through unconfined aquifers of finite base width

Figure 3 displays a typical longitudinal profile of an artificial cut with horizontal impermeable bedrock. The cut bottom coinciding with the bedrock is taken as a datum for the measurements of elevation ($Y = 0$). For a steady accretion-free flow, Equation (15) may be rewritten in the form:

$$\frac{\partial}{\partial x} \left(\frac{H^2}{2\Lambda} + \frac{H^3}{3\Lambda} H_{xx} \right) = -\frac{q}{K}. \quad (18)$$

Integrating the above expression with respect to x yields:

$$\frac{H^3}{3\Lambda} H_{xx} + \frac{H^2}{2\Lambda} = -\frac{q}{K} x + \omega_4, \quad (19)$$

where ω_4 is an integration constant and can be determined from the specified flow depth at the upstream end section ($j=0$) as a boundary condition. In practice, this section coincides with a groundwater divide or with a section where the horizontal Darcy velocity is almost negligible. Thus, the expression for ω_4 becomes:

$$\omega_4 = \frac{H_0^3}{3\Lambda_0} H_{xx,0} + \frac{H_0^2}{2\Lambda_0}. \quad (20)$$

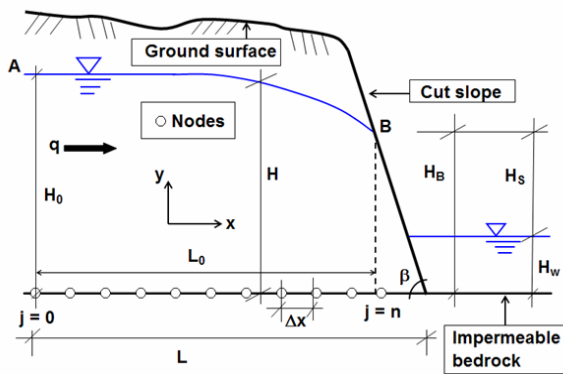


Figure 3: Definition sketch for unconfined seepage flow toward a highway cut slope.

Slika 3: Definijska skica za precejanje pri prosti gladini proti pobočju vkopa avtoceste.

In the above equation, the subscript 0 denotes flow parameters at the upstream end section. As discussed before, a numerical approach is the only way of obtaining a solution to Equation (19) for such a curvilinear potential-flow problem. The spatial derivative term of this equation is discretized using the four-point finite-difference equation (Bickley, 1941), which results in the following expression after some mathematical manipulation:

$$\begin{aligned} & \frac{H_j^3}{3\Lambda_j(\Delta x)^2}(H_{j+1} - 2H_j + H_{j-1}) + \frac{H_j^2}{2\Lambda_j} \\ & = -\frac{q}{K}(j\Delta x) + \frac{H_0^3}{3\Lambda_0}H_{xx,0} + \frac{H_0^2}{2\Lambda_0}, \end{aligned} \quad (21)$$

where Δx is the size of the step. With the aim of minimizing the numerical error due to spatial discretization, the step size is varied between 2 and 4% of the horizontal length of the model domain. For computational nodes near the downstream end, the derivative term is discretized with the three-point backward finite-difference approximation. Using the Newton–Raphson method with a numerical Jacobian matrix, the non-linear form of the algebraic equations is transformed into a linear one. The resulting implicit set of linear equations is then solved by means of the lower-upper (LU) decomposition method. A relative change in solution criterion with a tolerance of 10^{-6} is used for examining the convergence of the numerical solutions. More details regarding the applied numerical scheme can be found in Zerihun (2018).

3.1 Seepage discharge

Using the Darcy law, a general expression for the rate of seepage flow toward a highway cut slope with horizontal impermeable bedrock can be obtained as follows (Hantush, 1962; Polubarinova-Kochina, 1962, pp. 281-282; Kashef, 1969; Zerihun, 2018):

$$\begin{aligned} q &= \int_y^\eta u(y)dy = -K \int_y^\eta \frac{\partial \phi}{\partial x} dy \\ &= -K \frac{\partial}{\partial x} \left(\int_y^\eta \phi(y)dy - \frac{H^2}{2\Lambda} \right). \end{aligned} \quad (22)$$

As noted by Casagrande (1937) and Muskat (1946, p. 291), the terminal end of the phreatic-surface profile is tangent to the downstream face of the aquifer at the exit point B (see Figure 3). Using such a qualitative characteristic of the profile of the groundwater flow, the horizontal component of the phreatic-surface velocity at B was determined by applying the Darcy law. Utilizing this known velocity, Equation (22) was integrated between the vertical sections at $j=0$ and $j=n$ to give an expression for the seepage flux through a trapezoidal-shaped aquifer (for details, see the Appendix). The resulting equation for the seepage discharge reads as:

$$q = K \left(\frac{H_0^2 - \Gamma H_B^2}{2(L - H_B \cot \beta)} \right), \quad (23)$$

$$\Gamma = 1 - \frac{2}{3} \sin^2 \beta, \quad (24)$$

where β is the slope of the downstream face; H_B is the depth of the saturated aquifer at $j=n$; and L is the base width of the aquifer. Equation (23) is structurally similar to the discharge equation presented by Kashef (1969) after analyzing the hydrodynamic forces within the flow medium. This equation is directly coupled with Equation (19) for a complete numerical solution of the unconfined seepage-flow problem.

In the absence of tailwater, the maximum seepage discharge (Polubarinova-Kochina, 1962, p. 308; Kashef, 1969) can be obtained by differentiating Equation (23) with respect to H_B and equating the resulting expression to zero as follows:

$$\Gamma \cot \beta H_{mS}^2 - 2L\Gamma H_{mS} + H_0^2 \cot \beta = 0. \quad (25)$$

For a physically realistic solution, the discriminant of the above quadratic equation must be positive. Furthermore, its analytical solution satisfies the necessary condition $H_B < H_0$ and can be expressed as a non-dimensional form as follows:

$$\alpha_m = \frac{H_{mS}}{H_0} = \frac{\tan \beta}{\sigma} - \left(\frac{\tan^2 \beta}{\sigma^2} - \frac{1}{\Gamma} \right)^{1/2}, \quad (26)$$

where $\sigma (= H_0 / L)$ is the relative upstream depth of the saturated aquifer; H_{mS} is the maximum height of the seepage face for a downstream dry-bed condition; and α_m is the relative maximum seepage-face height. Using the above equation, an expression for H_0^2 as a function of L and β is obtained. Inserting this expression into Equation (23) leads to the following equation for the maximum seepage discharge:

$$q_m = \Gamma K H_{mS} \tan \beta, \quad (27)$$

where q_m is the maximum seepage discharge. Combining Equations (23) and (27) results in an expression for the relative seepage discharge as follows:

$$\Phi_R = \frac{q}{q_m} = \left(\frac{H_0}{H_{mS}} \right) \left(\frac{1 - \Gamma \alpha^2}{2\Gamma \left(\frac{\tan \beta}{\sigma} - \alpha \right)} \right), \quad (28)$$

where Φ_R is the relative seepage discharge, and $\alpha (= H_B / H_0)$ is the relative saturated depth of the aquifer at $j = n$. Using the definition of α in Equation (26), the resulting expression after simplification becomes:

$$\Omega_m = \frac{H_{mS}}{H_B} = \frac{\tan \beta}{\alpha \sigma} - \frac{1}{\alpha} \left(\frac{\tan^2 \beta}{\sigma^2} - \frac{1}{\Gamma} \right)^{1/2}, \quad (29)$$

where Ω_m is the ratio of the maximum seepage-face height to the downstream saturated depth in the presence of tailwater. As mentioned before, rigorous mathematical approaches have been previously employed to analyze unconfined seepage flows. For estimating the discharge, Pavlovsky (1931) (Polubarinova-Kochina, 1962, p. 306)

proposed an approximate equation, which is not a function of the downstream saturated depth, as follows:

$$q = \frac{\sigma K H_0}{1 + \sqrt{1 - \sigma^2 \cot^2 \beta}}. \quad (30)$$

For $\beta < 90^\circ$, Mikhailov (1952) systematically simplified the complex equation developed by Falkovich (Polubarinova-Kochina and Falkovich, 1951) and introduced a relatively simple equation as follows:

$$q = \frac{4KH_B}{\mu \cot \beta + 6 - \mu}, \quad (31)$$

where μ is a constant, and its value depends on the magnitude of $\cot \beta$. At the maximum seepage discharge, equating Equation (30) to Equation (31) and simplifying the resulting expression yields:

$$\alpha_m = \frac{H_{mS}}{H_0} = \frac{\sigma(\mu \cot \beta + 6 - \mu)}{4(1 + \sqrt{1 - \sigma^2 \cot^2 \beta})}, \quad (32)$$

which differs from Equation (26) by the additional parameter μ . Equations (30) and (32) are employed here to assess the performance of the proposed equations.

3.2 Effects of the downstream slope

As a part of this study, the effects of the downstream-face slope on the salient features of the unconfined seepage flow are examined. Figure 4a compares the predictions of Eq. (26) with the results of Eq. (32) for the relative maximum seepage-face height. As can be seen, the results of the proposed equation agree reasonably well with the results of the previous equation. For $\beta \geq 70^\circ$, some discrepancies can be seen between the results of the two equations, with a maximum absolute error of 3.6%. Considering the approximate nature of the simplified version of the previous equation, the performance of the proposed equation is satisfactory. For a constant σ , increasing the slope decreases the relative seepage-face height. This effect is significant for $\beta \leq 45^\circ$ and $\sigma > 0.10$. For a steeper slope, the variation of the relative seepage-face height with β is more gradual.

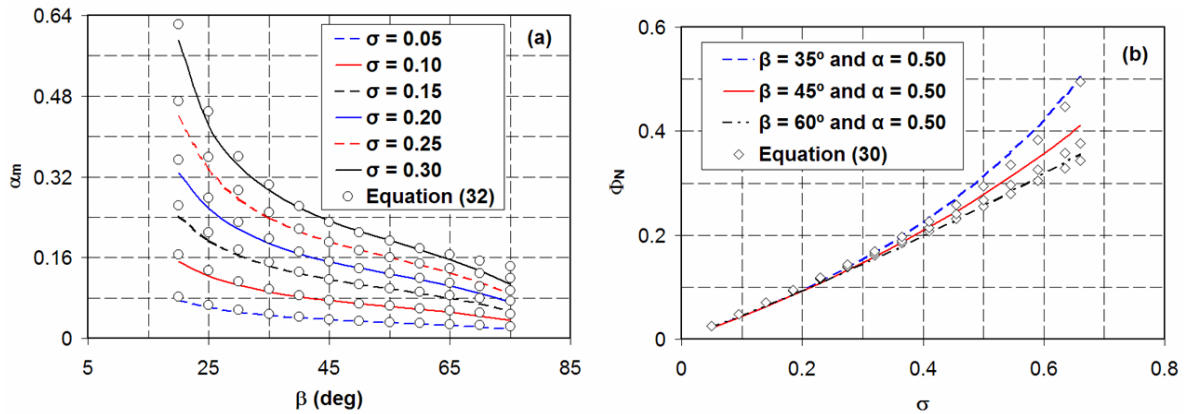


Figure 4: (a) Variation of the relative seepage-face height α_m with the slope of the downstream face β ; and (b) normalized seepage discharge Φ_N as a function of the relative upstream saturated depth σ . The results of Equations (26) and (23) in (a) and (b), respectively, are indicated by lines of different styles and colors.

Slika 4: (a) Sprememba relativne višine precejanja α_m z naklonom dolvodne meje β ; in (b) normaliziranega odtoka Φ_N kot funkcije relativne gorvodne zasičene globine σ . Rezultati enačb (26) in (23) v (a) oziroma (b) so označeni s črtami različnih slogov in barv.

The effect of the slope of the downstream face on the normalized seepage discharge $\Phi_N (= q / KH_0)$ is also examined, and the result is depicted in Figure 4b. The results of Equation (23) are favorably compared with the results of Equation (30). The computed maximum absolute error does not exceed 3.4% for numerical results with β values within the considered range. For $\sigma \leq 0.30$, the effect of the face slope on the normalized discharge is insignificant. For a relatively higher value, however, increasing the slope decreases the normalized discharge. This is due to the effect of β on the geometric characteristics of the phreatic-surface profile. The overall results revealed that the slope of the downstream face significantly affects both the relative seepage-face height and the normalized seepage discharge.

Likewise, the effect of the downstream-face slope on the relative seepage discharge is assessed using Equation (28). As shown in Figure 5, the reduction in seepage discharge decreases as β increases. For a larger face slope, the relative discharge varies more gradually with $1/\Omega_m$. Consequently, the drop in discharge is relatively small. For an artificial cut section with a flatter downstream-face slope, the converse is true. Apparently, the presence of

tailwater affects the height of the seepage face (H_S) and thus the relative discharge. The seepage-face height decreases with increasing tailwater depth ($H_S < H_{mS}$). As $\Omega_m \rightarrow 1$, the seepage discharge approaches the maximum value that corresponds to the condition of no tailwater. These results are consistent with previous results reported by Polubarinova-Kochina (1962, p. 308) for unconfined seepage flow through a triangular-shaped dam.

3.3 Phreatic-surface profile and piezometric head distributions

In this section, the model's accuracy is investigated by simulating unconfined seepage flow through a trapezoidal-shaped dam with vertical upstream and slanted downstream faces ($\beta = 45^\circ$). For this problem, the slope of the phreatic surface ($H_x = 0$) and the saturated depth were prescribed as boundary conditions at the upstream end section. The numerical technique applied here employs an iterative solution procedure based on the initial guess of the phreatic-surface profile. Using Equation (23), the discharge is first computed by utilizing the estimated depth of the saturated aquifer at $j = n$ ($H_B \leq H_{mS}$). If the discrepancy between

the H_B employed to compute q and the newly predicted H_B is significant, then the iteration process is continued until the discrepancy becomes insignificant (approximately less than 5 mm).

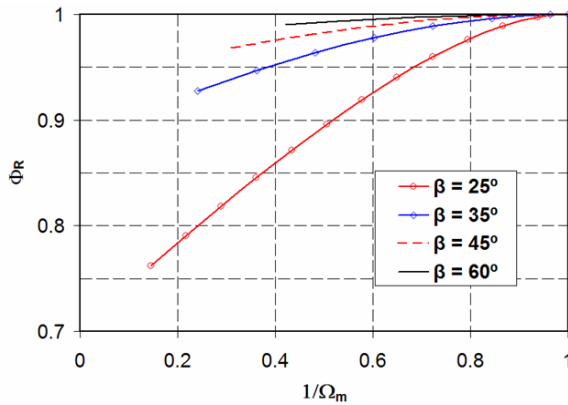


Figure 5: Variation of the relative seepage discharge Φ_R with the downstream saturated depth ratio $1/\Omega_m$ for various values of downstream-face slope.

Slika 5: Sprememba relativnega odtoka Φ_R z razmerjem dolvodne zasičene globine $1/\Omega_m$ za različne vrednosti naklona dolvodne meje.

The computational result of the present model was compared with the result of the finite-element numerical model (Lacy and Prevost, 1987) and the result of an approximate method that replaces the trapezoidal longitudinal section with an equivalent rectangular one (Kashef, 1969). According to this method, the locus of the phreatic surface is determined by:

$$\eta(x) = \left(H_0^2 \left(1 - \frac{2qx}{KH_0^2} \right) + \frac{1}{2} \left(\frac{q}{K} \right)^2 \left(1 - \exp \left(\frac{-4Kx}{q} \right) \right) \right)^{1/2} + Y, \quad (33)$$

$$\frac{q}{K} = \frac{H_0^2 - H_w^2}{2B_e}, \quad (34)$$

where H_w is the tailwater depth, and B_e is the width of the equivalent rectangular longitudinal section. The equation for the width of this section is

$$B_e = L - \frac{H_B \cot \beta}{2}. \quad (35)$$

As shown in Figure 6a, the result of the present model correlated reasonably well with the result of the finite-element numerical model with a mean relative error of 2.9%. Compared to these results, the approximate method underestimated the phreatic-surface elevations in the flow region near the sloping downstream face ($x/H_0 > 0.40$). Consequently, the exit point of the line of seepage and the curvature of the phreatic surface were not accurately predicted. The result of the test confirmed that the present model is capable of accurately simulating the flow pattern in the region where the streamline curvature and inclination are significant.

The results of the proposed model for the piezometric head distributions at vertical sections $x/H_0 = 0.18$, $x/H_0 = 0.38$, and $x/H_0 = 0.60$ were also compared with the solutions of the Kashef (1969) approximate method, which describes the vertical profile of the piezometric head by:

$$\phi = \phi_b + (H - \phi_b) \xi^2, \quad (36)$$

where ϕ_b is the piezometric head at the bedrock and can be determined from the following equation:

$$\phi_b = \frac{H}{4} + \frac{3H_0^2}{4H} \left(1 - \frac{x}{B_e} \right). \quad (37)$$

As shown in Figure 6b-d, the piezometric head at the bedrock decreases as the distance from the upstream end section increases. This is due to the effect of the vertical component of the flow, which is significant at a section near the discharge face.

Similar to its result for the phreatic-surface profile, the approximate method did not accurately simulate the distributions of the piezometric head. It underestimated the head at different levels, especially at a vertical section near the discharge face where a maximum discrepancy of 9.4% occurred. Compared to the results of the present model and the numerical data of Lacy and Prevost (1987), the conventional DF approach, which is based on an approximation of the hydrostatic pressure distribution, overestimated the distributions of the piezometric head throughout the computational domain, i.e., $\phi/\eta = 1.0$.

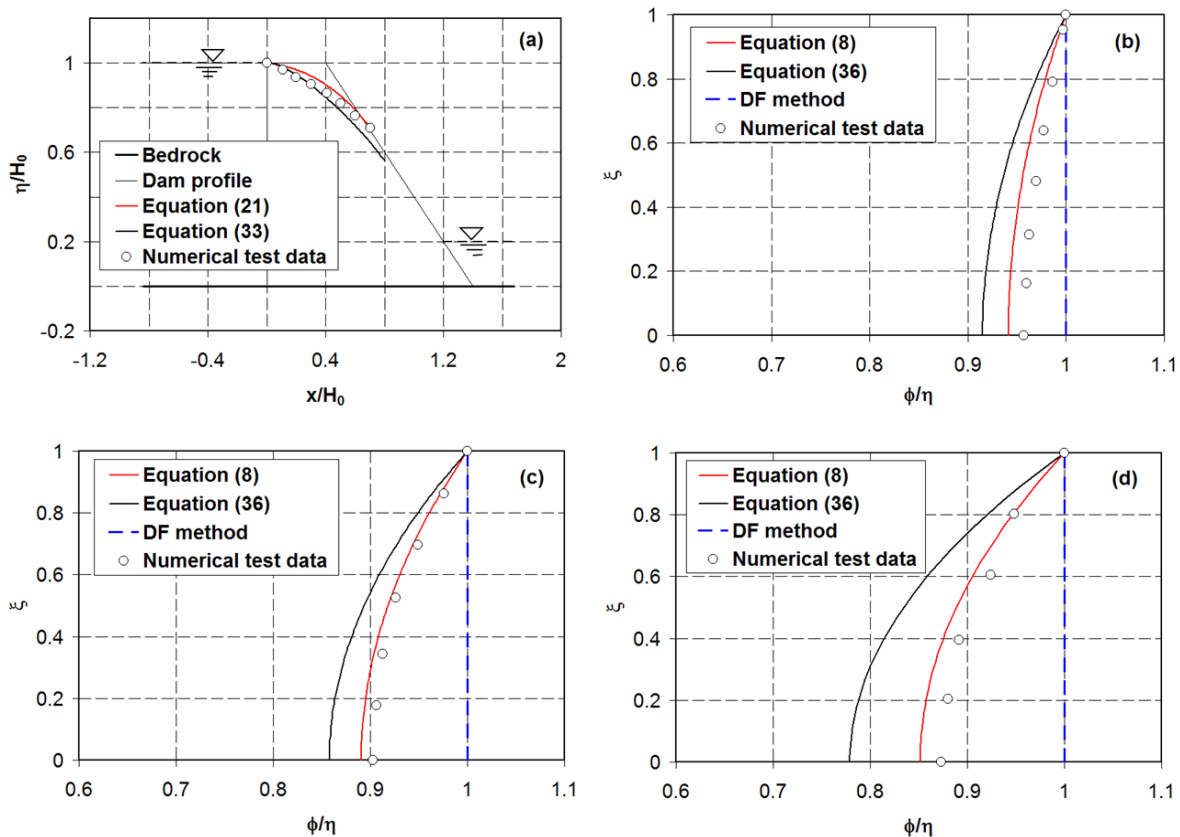


Figure 6: (a) Normalized phreatic-surface profile for curvilinear seepage flow ($\Phi_N = 0.47$). The normalized piezometric head distributions at vertical sections $x/H_0 = 0.18$, $x/H_0 = 0.38$, and $x/H_0 = 0.60$ are shown in (b), (c), and (d), respectively.

Slika 6: (a) Normaliziran profil gladine podzemne vode za ukrivljene tokovnice ($\Phi_N = 0.47$). Porazdelitve normalizirane hidravlične višine na navpičnih odsekih $x/H_0 = 0.18$, $x/H_0 = 0.38$ in $x/H_0 = 0.60$ so prikazane v (b), (c) oziroma (d).

4. Summary and conclusions

The problem of a steady-state phreatic flow through a homogeneous and isotropic aquifer with a slanting downstream face was investigated using a non-hydrostatic model. The proposed model incorporates a higher-order correction term, which accounts for the effects of the vertical component of the flow. Hence, it allows the treatment of complex unconfined flow behaviors that may influence the predictions of seepage discharge and seepage-face height, and overcomes the shortcomings of some of the existing models (e.g. Kashef, 1969; Chapman and Ong, 2006). A numerical approach based on the finite-difference approximations was employed for the solutions of the model equations. The model's capacity for analyzing the important features of the

seepage-flow problem was investigated by comparing its numerical results with the solutions of the full two-dimensional potential-flow method and rigorous mathematical approaches.

The following conclusions are drawn from this study:

1. The solutions of the proposed equations for the relative seepage-face height and the normalized seepage discharge qualitatively agreed with the results of the previous simplified equations. The result of the comparison is quite promising when considering the complex nature of the problem of seepage flow, where the vertical velocity plays a significant role. Overall, the investigation results confirmed that the

slope of the downstream face significantly affects both the relative seepage-face height and the normalized seepage discharge. Furthermore, the analysis of the relative discharge attested that the seepage discharge is strongly influenced by the downstream saturated depth ratio.

- For an unconfined seepage flow through a trapezoidal-shaped aquifer, the present model accurately reproduced the profile of the phreatic surface. In comparison, the Kashef (1969) approximate method underestimated the elevations of the phreatic surface in the flow region near the discharge face ($x/H_0 > 0.40$). The result of the comparison also revealed that the accuracy of the model predictions for the distributions of the piezometric head at different vertical sections is much better than the approximate method and the DF approach.

The test results presented in this study demonstrated the model's capability of yielding reasonably accurate solutions to the problems of the unconfined seepage flow. The good quality of the computational results may be attributed to the model's higher-order correction factor for the effects of the phreatic-surface curvature and steep slope. It is believed that the proposed model can serve as a numerical tool for solving engineering problems related to the stability analysis of a highway cut section and the design of the associated side channel.

Appendix: Discharge equation development

Along the streamline at the phreatic surface, if s is the local coordinate tangent to the phreatic surface and β is the angle between the streamline and the x -axis at B, then the expression for the Darcy velocity becomes (Harr, 1991, p. 68):

$$u_{p,B} = -K \frac{\partial \phi}{\partial x} = -K \frac{\partial \phi}{\partial s} \cos \beta \quad (38)$$

$$= K \sin \beta \cos \beta,$$

where $u_{p,B}$ is the horizontal component of the phreatic-surface velocity at B. For unconfined seepage flow through a trapezoidal-shaped aquifer with horizontal bedrock ($Y_x = Y_{xx} = Y_{xxx} = 0$), a general expression for the horizontal velocity at the phreatic surface, u_p , is obtained from Equations (14) and (15) as:

$$u_p = -KH_x(H_{xx}H + 1), \quad (39)$$

where H_x is the slope of the phreatic surface, which is equal to $-\tan \beta$ at B. Equating Equation (38) to Equation (39) gives the following expression:

$$H_{xx,B} = \frac{\cos^2 \beta - 1}{H_B} = \frac{-\sin^2 \beta}{H_B}. \quad (40)$$

Using the condition of a nearly hydrostatic flow at the upstream end section, Equation (22) is integrated between the vertical sections at $j=0$ and $j=n$. The resulting expression becomes:

$$\frac{qL_0}{K} = \frac{H_0^2}{2} - \frac{H_{xx,B}H_B^3}{3} - \frac{H_B^2}{2}, \quad (41)$$

$$L_0 = L - H_B \cot \beta, \quad (42)$$

where L_0 is the length of the projection of the phreatic-surface profile on the x -axis (see Figure 3). Substituting Equation (40) into Equation (41) and then simplifying the resulting expression gives the discharge equation for seepage flow as follows:

$$q = K \left(\frac{H_0^2 - \Gamma H_B^2}{2L_0} \right), \quad (43)$$

$$\Gamma = 1 - \frac{2}{3} \sin^2 \beta. \quad (44)$$

Notation

B_e	width of the equivalent rectangular-shaped aquifer [L]
g	gravitational acceleration [LT^{-2}]
h	vertical height above the bedrock [L]
H	depth of the saturated aquifer [L]
H_B	depth of the saturated aquifer at $j = n$ [L]
H_{mS}	maximum height of the seepage face [L]

H_S height of the seepage face [L]
 H_w tailwater depth [L]
 H_x , H_{xx} , and H_{xxx} derivatives of the saturated depth [-, L^{-1} , L^{-2}]
 H_0 saturated depth at the upstream end section [L]
 K hydraulic conductivity [LT^{-1}]
 L base width of the aquifer [L]
 L_0 length of the projection of the phreatic-surface profile on the x -axis [L]
 p pressure [$ML^{-1}T^{-2}$]
 q seepage discharge per unit width [L^2T^{-1}]
 q_m maximum seepage discharge [L^2T^{-1}]
 R rate of vertical recharge [LT^{-1}]
 s local coordinate tangent to the phreatic surface [L]
 t time [T]
 u horizontal velocity [LT^{-1}]
 u_p horizontal velocity at the phreatic surface [LT^{-1}]
 v vertical velocity [LT^{-1}]
 x , y , and z Cartesian coordinates [L]
 Y bedrock elevation [L]
 Y_x , Y_{xx} , and Y_{xxx} derivatives of the bedrock profile [-, L^{-1} , L^{-2}]
 α relative saturated depth at $j = n$ [-]
 α_m relative maximum seepage-face height [-]
 β slope of the downstream face [deg]
 γ unit weight of the fluid [$ML^{-2}T^{-2}$]
 Δx step size [L]
 η phreatic-surface elevation [L]
 λ effective porosity [-]
 μ a constant factor [-]
 ξ dimensionless vertical height [-]
 σ relative upstream saturated depth [-]
 ϕ piezometric head [L]
 ϕ_b piezometric head at the bedrock [L]
 Φ_N normalized seepage discharge [-]
 Φ_R relative seepage discharge [-]
 ψ stream function [L^2T^{-1}]
 ω_1 , ω_2 , and ω_3 functions of integration [L^2T^{-1}]

ω_4 an integration constant [L^2]
 Ω_m ratio of the maximum seepage-face height to the downstream saturated depth [-]

References

- Bear, J., Zaslavsky, D., Irmay, S. (1968) *Physical Principles of Water Percolation and Seepage*. Arid Zone Research - XXIX, UNSECO: Paris, France.
- Bear, J. (1988) *Dynamics of Fluid in Porous Media*. Dover Publications Inc.: Mineola, NY, USA.
- Bickley, W. G. (1941) Formulae for numerical differentiation. *Math. Gaz.*, 25(263), 19–27, <https://doi.org/10.2307/3606475>.
- Billstein, M. (1998) *Development of a Numerical Model of Flow through Embankment Dams*. Licentiate Thesis, Department of Environmental Engineering, Luleå University of Technology, Luleå, Sweden.
- Boussinesq, J. (1871) Théorie de l'intumescence liquide appelée onde solitaire ou de translation, se propageant dans un canal rectangulaire (Theory of liquid wave referred to as a solitary or a translation wave, propagating in a rectangular canal). *Comptes Rendus, Académie des Sciences*, 72, 755–759 [in French].
- Casagrande, A. (1937) Seepage through dams. *J. New England Water Works Assoc.*, **51**(2), 131–172.
- Castro-Orgaz, O., Hager, W. H. (2014) One-dimensional modeling of curvilinear free-surface flow: Generalized Matthew theory. *J. Hydraul. Res.*, **52**(1), 14–23. <https://doi.org/10.1080/00221686.2013.834853>.
- Chapman, T. G. (1980) Modeling groundwater flow over sloping beds. *Water Resour. Res.*, **16**(6), 1114–1118. <https://doi.org/10.1029/WR016i06p01114>.
- Chapman, T. G., Dressler, R. F. (1984) Unsteady shallow groundwater flow over a curved impermeable boundary. *Water Resour. Res.* **20**(10), 1427–1434. <https://doi.org/10.1029/WR020i010p01427>.
- Chapman, T. G., Ong, G. (2006) A new equation for shallow groundwater flow over a curved impermeable boundary: Numerical solutions and laboratory tests. *Water Resour. Res.*, **42**, W03427, <https://doi.org/10.1029/2005WR004437>.
- Childs, E. C. (1971) Drainage of groundwater resting on a sloping bed. *Water Resour. Res.*, **7**(5), 1256–1263. <https://doi.org/10.1029/WR007i005p01256>.

- Dagan, G. (1967) Second-order theory of shallow free-surface flow in porous media. *Q. J. Mech. Appl. Math.*, **20**, 517–526. <https://doi.org/10.1093/qjmam/20.4.517>.
- Di Nucci, C. (2018) Unsteady free-surface flow in porous media: One-dimensional model equations including vertical effects and seepage face. *C. R. Mecanique*, **346**, 366–383.
- Dupuit, J. (1863) *Études Théoriques et Pratiques sur le Mouvement des Eaux dans les Canaux Découverts et a Travers les Terrains Perméables (Theoretical and Practical Studies on Water Movement in Open Channels and across Permeable Terrains)*. deuxième édition; Dunod: Paris, France, 229–293 [in French].
- Forchheimer, P. (1886) Über die ergieblgkeit von brunnenanlagen und sickerschlitzen (On the productivity of well systems and seepage slits). *Zeitschnft des Archttekten und Ingcnieurvereins zu Hannover*, **32(7)**, 538–564 [in German].
- Forchheimer, P. (1914) *Hydraulik (Hydraulics)*. 1st ed.; Druck und Verlag Von B. G. Teubner: Leipzig und Berlin, Germany, 420–467 [in German].
- Fukuchi, T. (2018) New high-precision empirical methods for predicting the seepage discharges and free-surface locations of earth dams validated by numerical analyses using the IFDM. *Soils Found.*, **58**, 427–445.
- Hall, H. P. (1955) An investigation of steady flow toward a gravity well. *La Houille Blanche*, **10(1-2)**, 8–35.
- Hantush, M. S. (1962) On the validity of the Dupuit–Forchheimer well-discharge formula. *J. Geophys. Res.*, **67(6)**, 2417–2420. <https://doi.org/10.1029/JZ067i006p02417>.
- Harr, M. E. (1991) *Groundwater and Seepage*. Dover Publications Inc.: Mineola, NY, USA.
- Hilberts, A. G. J., von Loon, E. E., Troch, P. A., Paniconi, C. (2004) The hillslope-storage Boussinesq model for non-constant bedrock slope. *J. Hydrol.*, **291**, 160–173. <https://doi.org/10.1016/j.jhydrol.2003.12.043>.
- Kacimov, A., Obnosov, Y. (2012) Analytical solutions for seepage near material boundaries in dam cores: The Davison–Kalinin problems revisited. *Appl. Math. Model.*, **36**, 1286–1301. <https://doi.org/10.1016/j.apm.2011.07.088>.
- Kashef, A. I. (1969) Groundwater movement toward artificial cuts. *Water Resour. Res.*, **5(5)**, 1032–1040. <https://doi.org/10.1029/WR005i005p01032>.
- Knight, J. H. (2005) Improving the Dupuit–Forchheimer groundwater free-surface approximation. *Adv. Water Resour.*, **28(10)**, 1048–1056. <https://doi.org/10.1016/j.advwatres.2005.04.014>.
- Kozeny, J. (1931) Grundwasserbewegung bei freiem Spiegel, Fluss und Kanalversickerung (Groundwater movement at free level, River and Channel Infiltration). *Wasserkraft und Wasserwirtschaft*, **26(3)**, 28–31 [in German].
- Lacy, S. J., Prevost, J. H. (1987) Flow through porous media: A procedure for locating the free surface. *Int. J. Numer. Anal. Meth. Geomech.*, **11**, 585–601. <https://doi.org/10.1002/nag.1610110605>.
- Matthew, G. D. (1991) Higher order, one-dimensional equations of potential flow in open channels. *Proc. Instn. Civ. Eng.*, **91(3)**, 187–201. <https://doi.org/10.1680/icep.1991.14974>.
- Mikhailov, G. K. (1952) *Concerning the Seepage in Trapezoidal Dams on Horizontal Bedrock*. *Gidrotekhnika i Melioratsiya*, No. 1, USSR [in Russian].
- Muleshkov, A. and Banerjee, S. (1987) Seepage towards vertical cuts. *J. Geotech. Eng.*, **113(12)**, 1419–1431. [https://doi.org/10.1061/\(ASCE\)0733-9410\(1987\)113:12\(1419\)](https://doi.org/10.1061/(ASCE)0733-9410(1987)113:12(1419)).
- Muskat, M. (1946) *The Flow of Homogeneous Fluids through Porous Media*. J. W. Edwards, Inc.: Ann Arbor, MI, USA.
- Pavlovsky, N. N. (1931) *On Seepage through Earth Dams*. Instituta Gidrotekhniki i Melioratsii, Leningrad, USSR [in Russian].
- Polubarinova-Kochina, P. Ya., Falkovich, S. B. (1951) Theory of filtration of liquids in porous media. In: *Advances in Applied Mechanics*, von Mises, R. and von Kármán, T. (eds.), Academic Press, New York, NY, USA, **2**, 153–225.
- Polubarinova-Kochina, P. Ya. (1962) *Theory of Groundwater Movement*. Princeton University Press: Princeton, NJ, USA.
- Rayleigh, L. (1876) On waves. *Phil. Mag.*, **1(4)**, 257–279. Available online: <http://archive.org/details/londonedinburgh511876lond> (accessed on 10 November 2022).
- Vauclin, M., Khanji, D., Vachaud, G. (1979) Experimental and numerical study of a transient, two-dimensional unsaturated-saturated water table recharge problem. *Water Resour. Res.*, **15(5)**, 1089–1101. <https://doi.org/10.1029/WR015i005p01089>.
- Zerihun, Y. T. (2018) Extension of the Dupuit–Forchheimer model for non-hydrostatic flows in

unconfined aquifers. *Fluids*, **3(2)**,
<https://doi.org/10.3390/fluids3020042>.

Zerihun, Y. T. (2020) A numerical investigation of transient groundwater flows with a phreatic surface along complex hillslopes. *Slovak J. Civ. Eng.*, **28(1)**, 11–19.
<https://doi.org/10.2478/sjce-2020-0002>.